Advances in Science and Technology Research Journal

Advances in Science and Technology Research Journal 2022, 16(5), 216–229
https://doi.org/10.12913/22998624/154792
ISSN 2299-8624, License CC-BY 4.0

Received: 2022.07.25
Accepted: 2022.10.17
Published: 2022.11.01

The Influence of Natural Aging of the $AlCu_4Mg_1$ Aluminum Sheet Alloy on the Constitutive Parameters of Selected Models of Flow Stress

Stanisław Kut[1*], Grzegorz Pasowicz[2], Feliks Stachowicz[1]

[1] Rzeszow University of Technology, al. Powstańców Warszawy 12, 35-959 Rzeszów, Poland

[2] Doctoral School of Engineering and Technical Sciences at the Rzeszow University of Technology, al. Powstańców Warszawy 12, 35-959 Rzeszów, Poland

* Corresponding author's e-mail: stan_kut@prz.edu.pl

ABSTRACT

This paper presents the results of experimental studies aimed at determining constitutive parameters for selected constitutive equations of flow stress as a function of the natural aging time of 2 mm thick AlCu4Mg1 (AW-2024) sheet. The knowledge of these constitutive parameters as a function of aging time is necessary to analyze and model the processes of forming sheet metal stampings after heat treatment during natural aging. The constitutive parameters in individual constitutive equations were determined on the basis of the approximation of the course of strain hardening curves. The courses of these curves for the tested natural aging times in the range of 0–120 minutes after heat treatment were made on the basis of uniaxial stretching tests of samples taken in the directions of 0°, 45° and 90° to the direction of sheet rolling. The values of constitutive parameters as a function of natural aging time were determined for four popular models of flow stress: Hollomon, Swift, Voce and El-Magd. Moreover, the relationship between the natural aging time and the value of the yield strength in the tested aging time range was determined, and the accuracy of the investigated constitutive equations for describing the course of the flow stress of the tested sheet material was assessed on the basis of the analysis of approximation errors.

Keywords: AW-2024 sheet, natural aging, uniaxial tensile tests, flow stress models, constitutive parameters.

INTRODUCTION

Aluminum alloys, due to their properties (including high strength-to-weight ratio) and well-mastered ability to produce them, are widely used in aviation and other areas of the transport industry [1]. Currently, apart from composite materials, their percentage share is the largest in the production of aircraft. A practical example of this is AlCu4Mg1 alloy. Its precipitation hardening ability is very often used to achieve the required mechanical properties [2,3]. After solution treatment (heat treatment and aging), it shows relatively high strength and good fracture toughness [4–6]. Aging after heat treatment may be natural or accelerated (artificial aging) [7, 8]. Natural aging usually gives better results in the form of increasing the strength of the drawpiece material than accelerated aging, but it lasts much longer, i.e., 4–5 days [8]. On the other hand, an increase in temperature causes a decrease in the accelerated aging time. Unfortunately, the material strength gets reduced after aging [7, 8].

In industrial practice, aluminum sheet drawpieces pressings with the ability to harden precipitation can be shaped in two variants (Fig. 1). In the first one, the sheets are shaped after softening annealing in the so-called "0" state, while the finished drawpieces undergo heat treatment and aging. On the other hand, in the second variant, the sheets are shaped after heat treatment. Forming the sheet after heat treatment is advantageous because the drawpiece does not enter the furnace after forming, where it could deform during the heat treatment process by heating in the furnace followed by rapid cooling. Moreover, which is also very favorable, it is much easier to perform heat treatment of the sheets in the form of flat sheets than in the form of moldings formed therefrom with complex shapes.

However, after heat treatment during natural aging, there is an increase in strength and a decrease in deformability of the sheet material, which is unfavorable from the point of view of technological properties [9]. The work [10] presents the results of research on the variability of the microstructure as well as the strength and plastic properties of AW-2024 sheet 0.81 mm thick immediately after heat treatment and during natural aging for a specified time (0.5, 1.5, 4 and 24 hours) after heat treatment. The obtained results indicate that the greatest increase in strength properties occurred during natural aging up to 4 hours after heat treatment. For example, after 4 hours of aging, the yield strength value increased by approx. 86% compared to the yield strength immediately after heat treatment. However, in the tested time from 4 to 24 hours, the increase in the yield strength was not so intense and amounted to only about 20% compared to the yield strength after 4 hours of natural aging. Thus, the greatest increase in the strength properties and the simultaneous decrease in deformability of the material occur in the first hours after heat treatment, i.e., the time when the drawpieces according to the second variant are formed, i.e., from

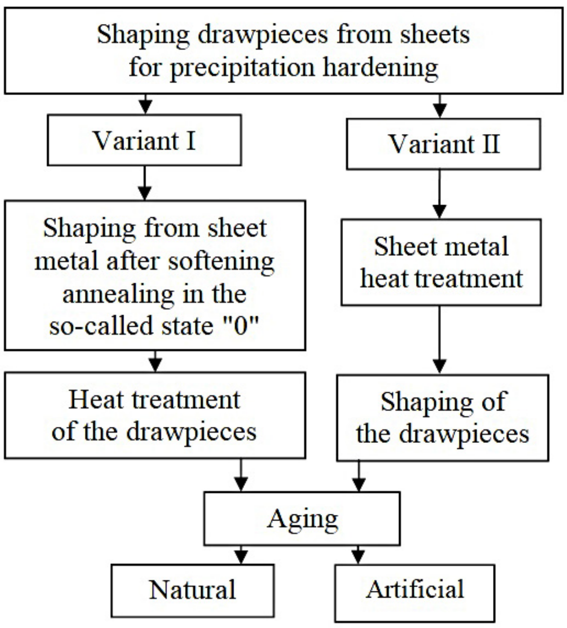

Fig. 1. Variants of forming drawpieces from aluminum sheets for precipitation hardening

sheet metal after heat treatment. Therefore, the parameters of the drawpieces shaping process (e.g., forming forces, susceptibility to plastic deformation) and the behavior of the material in this process (e.g., the amount of springback of the sheet) will significantly depend on the time after heat treatment in which a given technological operation will be carried out.

Due to the above, in engineering practice, forming sheet metal elements in the second variant, i.e., after heat treatment, requires taking into account the technological process called stamping. Changes in the properties of the sheet material occur as a result of natural aging at subsequent stages of the technological process. For this purpose, it is necessary to know the strength and plastic parameters as well as the constitutive parameters in the constitutive equations of the flow stress function depending on the natural aging time after heat treatment.

The process of aging the sheet material after heat treatment can be slowed down or delayed by lowering the temperature, which creates conditions for the industrial implementation of the processes of shaping stampings from heat treatment sheets. The work [9] presents, inter alia, the results of research on the influence of the storage time in the freezer of sheet metal after heat treatment on its strength and plastic properties. The tests were carried out with the use of 2 mm thick AW-2024 sheet, which was stored in a freezer at -15 °C after heat treatment. Then, after 72, 120, 168 and 240 hours of storage in the freezer, uniaxial tensile tests were carried out in order to determine the strength and plastic properties. For the storage time in the freezer from 3 to 10 days, an almost 5% increase in the yield strength was observed. At the same time, the percentage permanent elongation at maximum force A_g and percentage elongation after fracture $A_{80\ mm}$ practically did not change. It is advantageous because storing the sheet in a freezer after heat treatment gives some possibilities related to the preparation and implementation of the entire technological and production process of sheet metal parts shaped in the second variant, i.e., after heat treatment. In industrial practice, the possibility of storing sheets after heat treatment in a freezer allows the process of forming a given batch of parts at a given production station at the same time after removal from the freezer, i.e., at the same stage of natural aging, which ensures repeatability of the technological properties of the charge sheet.

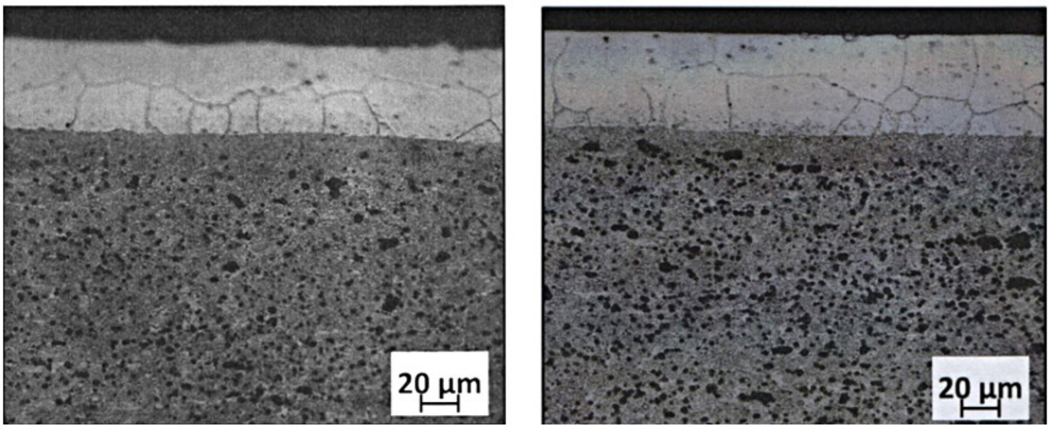

Fig. 2. Microstructure of the tested sheet in the longitudinal direction (left) and in the transverse direction (right) according to the rolling direction

For this reason, during designing and analyzing the technological process of the drawpiece, it is important to determine at what stage of aging after heat treatment a specific operation of plastic forming of the part will be performed and to know the constitutive parameters for this stage in the constitutive equations of flow stress.

As already mentioned, the analysis and design of the technological process of the sheet metal stamping after heat treatment requires, first of all, the knowledge of the constitutive parameters in the constitutive equations of flow stress as a function of natural aging time. Unfortunately, there are no studies in this field in the literature, which was the basis for the research presented in this paper.

The aim of the research presented in this paper was to determine the constitutive parameters for AW-2024 sheet with a thickness of 2 mm as a function of the natural aging time after heat treatment for four selected constitutive models of flow stress. Moreover, on the basis of the analysis of approximation errors, an assessment of the suitability of the four tested models was made to describe the course of the deformation hardening curves of the material of the tested sheet after heat treatment and during natural aging. Changes in the material properties of the shaped sheet result from natural aging after heat treatment. The experimentally determined values of constitutive parameters as a function of aging time will make it possible to take into account the changes in the material properties of the shaped sheet.

TEST MATERIAL AND EXPERIMENTAL PROCEDURE

The tested material was a 2 mm thick AlCu4Mg1 (AW-2024) aluminum alloy clad sheet. The microstructure of the tested sheet in the delivery condition, i.e. after softening annealing with the visible layer of the plating, is shown in Figure 2. No significant differences were found between the microstructure of the specimens taken in the longitudinal and transverse directions in relation to the rolling direction of the sheet, which results from the softened state of the material, coagulation of precipitates and no granular structure. The thickness of the plating layers was 5.5% of the total sheet thickness. The chemical composition of the tested sheet material is presented in Table 1.

From this sheet as delivered, i.e., after softening annealing, samples were taken for uniaxial stretching in the directions 0^{o}, 45^{o} and 90^{o} to the direction of sheet rolling. A total of 45 samples were prepared for the five aging time measurement points. The shape and dimensions of samples for testing in accordance with ISO 6892-1 are shown in Figure 3

Table 1. Chemical composition of tested sheet material [11]

Si	Fe	Cu	Mn	Mg	Cr	Zn	Ti	Zr+Ti	Others		Aluminum min.
									Each	Total	
≤0.5	≤0.5	3.8–4.9	0.3–0.9	1.2–1.8	≤0.1	≤0.25	≤0.15	≤0.2	0.05	0.15	Remainder

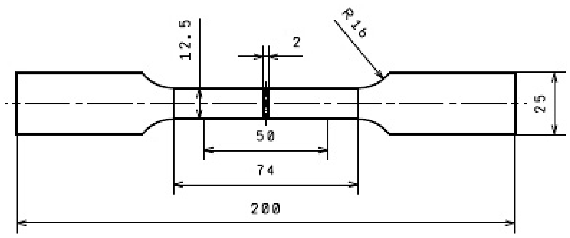

Fig. 3. Shape and dimensions of test specimens in mm

Heat treatment was carried out on the prepared samples. The samples were successively heated in an oven to the temperature of 493 °C and kept at this temperature for 40 minutes [12], and then subjected to rapid cooling in cold water. Then, uniaxial tensile tests were carried out successively immediately after heat treatment and during natural aging for 0, 20, 45, 90 and 120 minutes after heat treatment. The tensile speed of the samples was 30 mm / min. The scope of aging time covered by the study was determined on the basis of an analysis of the range of manufactured drawpieces and engineering practice, taking into account the AMS2770 standard [12]. The time determined in this way was considered fully sufficient to complete the required technological operations of forming sheet metal parts.

Fig. 4. An example of a sample during the uniaxial tensile test

Such a time range was considered to be fully sufficient to carry out the required technological operations of shaping sheet metal parts. For each of the tested aging times after heat treatment, three samples were stretched in each direction. For this reason, in order to maintain the assumed time intervals between individual tests, solution heat treatment, and then uniaxial tensile tests were carried out in three rounds of 15 samples each. Static uniaxial tensile tests of individual samples were carried out successively on the Zwick / Roell Z030 testing machine with measurement of the elongation and change of the sample width using a multiexstensometer (Fig. 4).

RESULTS AND DISCUSSION

On the basis of the obtained results of experimental tests, the curves of strain hardening for particular directions 0, 45 and 90° according to rolling direction and five times after heat treatment were developed. Then, the values of material coefficients were determined for four selected constitutive models of flow stress. For individual constitutive models, the values of the errors in fitting the strain hardening curves were calculated. Based on the analysis of these errors, the most favorable model for describing the material of the tested sheet was identified. Moreover, the influence of time after heat treatment on the value of the yield strength in the tested aging time was analyzed.

Influence of natural aging time on the yield strength

The yield strength is one of the basic strength parameters of the material, the numerical value of which significantly affects not only the forming forces and tool load, but also other parameters of the technological process, such as the amount of springback of the sheet. Therefore, it is important to know how this parameter changes with the aging time after heat treatment. The diagram (Fig. 5) shows the dependence of the yield strength of the tested sheet material as a function of the natural aging time after heat treatment. The numerical values for individual experimental points in the graphs present the arithmetic mean value obtained on the basis of three uniaxial stretching tests carried out in the same conditions. The obtained test results showed some differentiation of the strength and plastic properties of the tested sheet depending on the direction of sample collection (average normal anisotropy $\bar{r} = 0.73$ and its value practically did not depend on the aging time). The highest values of the yield point were in the 0° direction, slightly lower in the 90° direction, and the lowest in the 45° direction towards the rolling direction. In all directions, an almost linear increase in the yield strength was observed as a function of the natural aging time over the entire tested time range, i.e., 0–120 minutes. An approx. 43% increase in the yield point was observed. The position of the points on the graphs for the average value of individual parameters [$R_{p0.2\text{-AV}}$, $B_{d\text{-}AV}$, $n_{1\text{-}AV}$, $K_{2\text{-}AV}$, $n_{2\text{-}AV}$, $\varepsilon_{0\text{-}AV}$, $A_{3\text{-}AV}$, $K_{3\text{-}AV}$, $n_{3\text{-}AV}$, $A_{4\text{-}AV}$, $B_{4\text{-}AV}$, $K_{4\text{-}AV}$] described later in the paper were calculated on the basis of the results for samples with different orientations in relation to the rolling direction according to the relationship:

$$X_{AV} = (X_0 + 2X_{45} + X_{90})/4 \quad (1)$$

where: X – the parameter, the subscripts denote the orientation of the specimen with respect to the rolling direction of the sheet.

As a result of the approximation of the experimental points, linear equations were obtained describing the increase in the yield point as a function of the natural aging time in particular directions. These equations for individual directions [$R_{p0.2\text{-}0}$(t), $R_{p0.2\text{-}45}$(t), $R_{p0.2\text{-}90}$(t))] and for the average value [$R_{p0.2\text{-AV}}$(t)], were in the diagram (Fig. 5). In all cases, the correlation coefficient $R^2 > 0.99$.

Influence of natural aging time on strain hardening curves

The hardening curves reflect the behavior of the material during plastic deformation. Their course describes the change in flow stress σ_p as a function of plastic strain ε_p. They are usually determined on the basis of uniaxial tensile, compression and torsion tests. Knowledge of the hardening curves is of great practical importance and is necessary for mathematical modeling of plastic working processes.

The graph (Fig. 6) shows the experimentally determined curves of the material hardening of the tested sheet in the 0° direction for the tested times after heat treatment. On the other hand, in the graphs (Figs. 7 and 8), the curves of the strain hardening curve determined in the directions 45° (Fig. 7) and 90° (Fig. 8) for the same times after heat treatment. In all cases, a clear influence of the aging time on the course of the hardening curve was observed, with the aging time increasing the value of the flow stress σ_p proportionally over the entire range of plastic strain ε_p.

Selected models of flow stress

For practical reasons, the curves of strain hardening are presented in the form of constitutive equations of the so-called function of flow stress. Such equations are used, inter alia, for the analysis and simulation of cold forming processes at relatively low strain rates, when their influence on the flow stress can be neglected. In this paper, four models of flow stress of various complexity

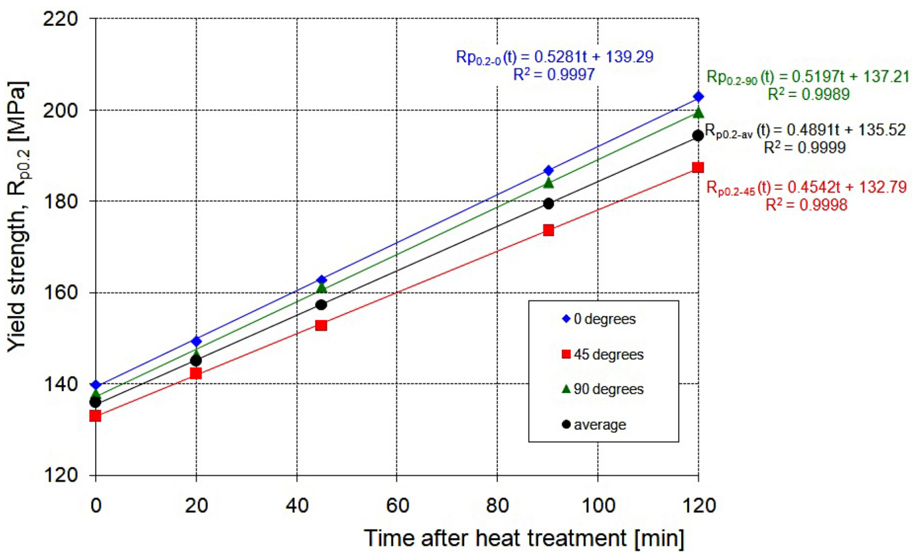

Fig. 5. Influence of aging time on the yield strength

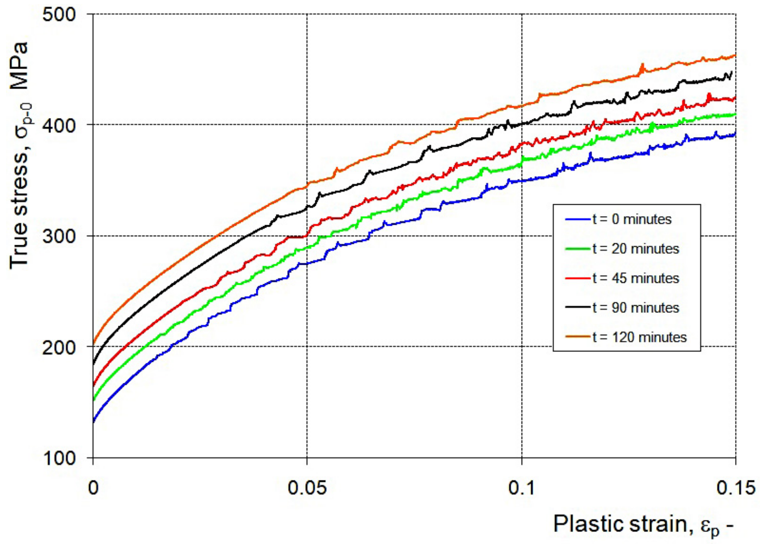

Fig. 6. Strain hardening curves in the direction of 0° for the five tested times after heat treatment

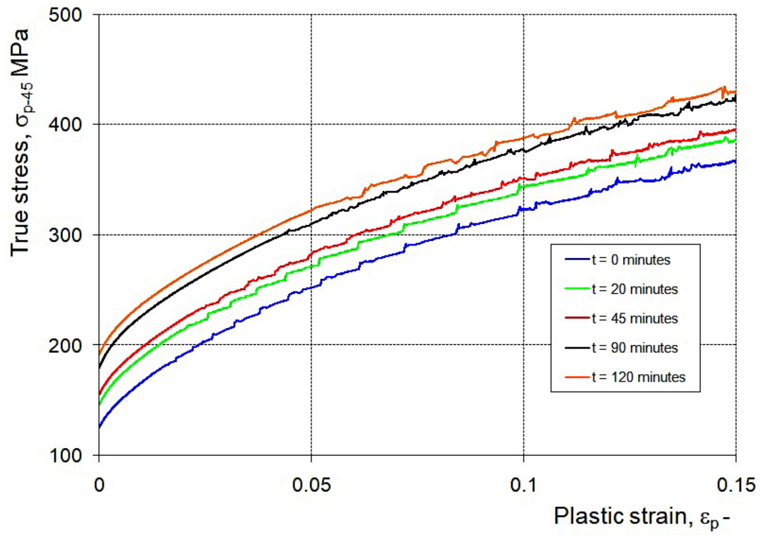

Fig. 7. Strain hardening curves in the direction of 45° for the five tested times after heat treatment

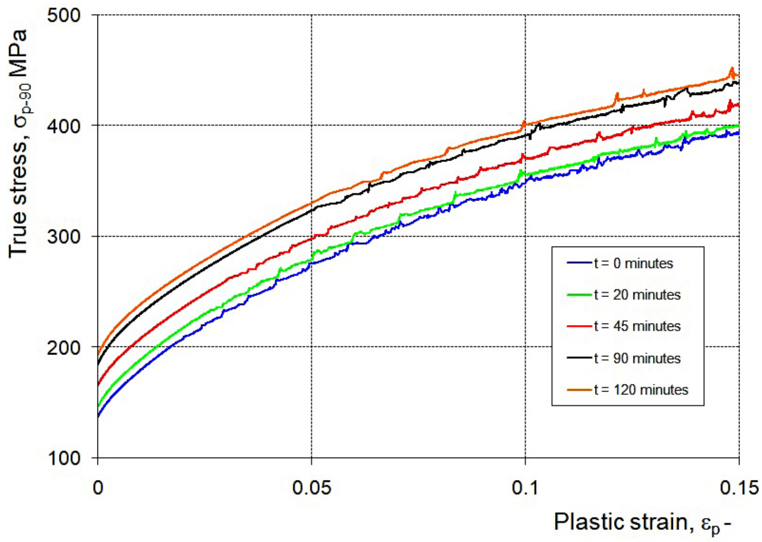

Fig. 8. Strain hardening curves in the direction of 90° for the five tested times after heat treatment

levels were selected to describe the course of the material strain hardening of the tested sheet:

I. Hollomon [13]

$$\sigma_p(\varepsilon_p) = K_1 \varepsilon_p^{\,n_1} \quad (2)$$

II. Swift [14]

$$\sigma_p(\varepsilon_p) = K_2(\varepsilon_0 + \varepsilon_p)^{n_2} \quad (3)$$

III. Voce [15]

$$\sigma_p(\varepsilon_p) = A_3 + K_3(1 - \exp(-n_3 \varepsilon_p)) \quad (4)$$

IV. El-Magd [16]

$$\sigma_p(\varepsilon_p) = A_4 + B_4 \varepsilon_p + K_4(1 - \exp(-n_4 \varepsilon_p)) \quad (5)$$

where: σ_p – flow stress,
ε_p – equivalent plastic strain,
$K_1 \div K_4, A_3, A_4, B_4, \mathcal{E}_0, n_1 \div n_4$ – constitutive parameters determined experimentally.

The Hollomon model is the simplest and most often used in engineering practice, the strain hardening model, which provides a good description of the hardening curve in a wide range of deformation, which is why it is willingly used in modeling plastic forming processes, especially those with large deformations, such as forging, extrusion, punching, etc. The Swift model, like the Hollomon model, due to its versatility but also greater accuracy in the description of the initial course of the strain hardening curve, is very often used in numerical modeling of a wide range of plastic forming processes in the field of small and large deformations. Voce is also often used to describe the course of the strain hardening curve, which, like the Swift model, requires knowledge of three constitutive parameters. The most complex of the selected models is the El-Magd model. This is extended Voce model with an additional linear component, and its use requires the determination of as many as four constitutive parameters. In the literature, El-Magd model is also referred to as the extended Voce model [17].

Influence of constitutive equation on the error of matching curves of strain hardening

The material constants in equations 2–5 were determined for the individual strain hardening curves using the least squares method using the Logger Pro program. The error of fit B_d was calculated by relating the root mean square error RMSE to the mean feature level σ_p from the relationship:

$$B_d = \frac{RMSE}{(\sigma_p)_{av}} \cdot 100\% \quad (6)$$

The graph (Fig. 9) presents the mean values of the error in matching the course of the strengthening curves for each constitutive model. The average error of fit for individual models was calculated from the dependence (1) on the basis of the values of the errors of fit calculated in the 0, 45 and 90° directions to the rolling direction. The largest mean error of fit in the range (1.6–1.8%) was shown by the Hollomon model, with a slight decrease in the value of this error with the aging time. In the case of the Swift model, the mean error of fit immediately after heat treatment was 1.1% and it decreased with the aging time reaching the value of 0.67% for the 120 minutes aging time. Only slightly lower values of the mean error of fit were obtained for the Voce model, but the mean error of fit after heat treatment was 0.67% and (unlike the Swift model) it increased to 0.87% for the time of 120 minutes. In the case of the Voce model, the value of the fit error practically did not depend on the aging time and amounted to approx. 0.83%. The smallest error of fit occurred with the use of the El-Magd model and amounted to approx. 0.67%. As in the case of the Voce model, the value of the error of fit using the El-Magd model was practically constant regardless of the test time after heat treatment. The analysis of the error of fit results shows that models in which the value of the fit error is the smallest and practically does not depend on the aging time will be the most favorable for describing the yield stress of the tested sheet material in the scope of the tested aging times. These criteria are best met by the El-Magd model. The Voce model was only slightly worse in this comparison.

Parameters in constitutive equations as a function of aging time

In order to determine the dependence of the effect of the natural aging time after heat treatment on the value of the constitutive parameters in equations 2–5, graphs were prepared

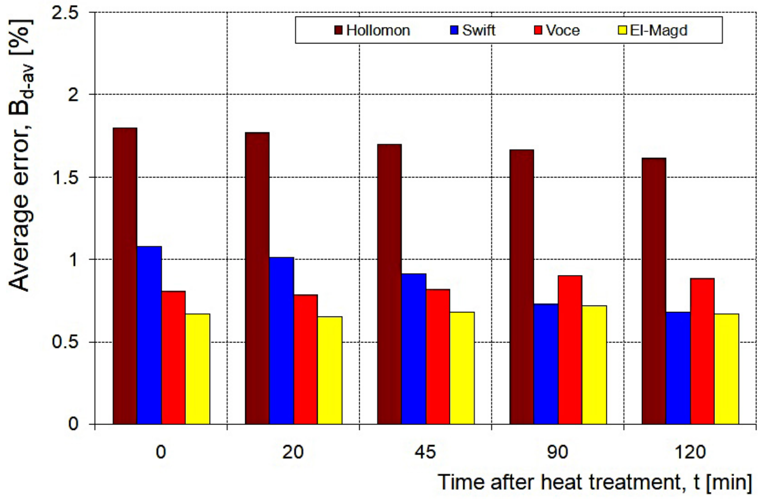

Fig. 9. Average matching error of curve for the tested models

showing the dependence of individual coefficients as a function of the aging time after heat treatment. The points on the graphs for the 0, 45 and 90° directions (Fig. 10–21) represent the arithmetic average value of a given material factor, calculated on the basis of the approximation of the strain hardening curves for three tensile tests carried out under the same conditions. On the other hand, the location of the points for the average values of individual material parameters in these charts was calculated from the dependence (1).

In the case of the K_1 and K_2 parameters in the Hollomon and Swift equations (Figs. 10 and 12), no specific trend was observed in aging after heat treatment in any of the directions. For this reason, the values of these parameters were assumed to be constant in the range of the investigated heat treatment time, and their average value for each direction was calculated on the basis of five measurement points and presented in these graphs. On the other hand, a clear influence of the aging time was observed for the exponents of the strain hardening curves n_1 and n_2, respectively, in these equations (Figs. 11 and 13). In the case of these parameters in all directions, a decrease in their value was observed with the aging time, and the trend was practically linear. As a result of the approximation of the experimental points with linear equations, the values of the constitutive parameters in these equations were determined, which were presented in the graphs (Fig. 11 and 13) together with the values of the correlation coefficient R^2. In the case of the exponents n_1 and n_2, there was a high correlation, and the correlation coefficient for the average values of these coefficients was $R^2 > 0.99$. Among the respondents, only the parameters ε_0 in the Swift equation did not show a typical linear trend. Therefore, in this case, the nonlinear equation presented in the graph was used for approximation (Fig. 14). In this case, the matching error for the average value $\varepsilon_{0\text{-AV}}$ calculated from the dependence (6) was 0.3%.

In the case of the Voce model and the El-Magd model, the material coefficients showed an almost linear relationship in the tested aging time after heat treatment (Figs. 15–21). However, in the case of the A_3 and n_3 coefficients (Figs. 15 and 17), as well as A_4, B_4 and n_4 (Figs. 18, 19 and 21), an increase in their values was observed during aging after heat treatment. However, in the case of the remaining material coefficients K_3 (Fig. 16) and K_4 (Fig. 20), a decrease in their values was observed over time after heat treatment. As above, the calculated values of the coefficients in the linear equations and the value of the correlation coefficient R^2 for each coefficient are presented in the form of equations in the graphs (Figs. 15–21).

The most important from the point of practical use of individual constitutive equations (e.g., in numerical modeling of the processes of forming the tested sheet metal after heat treatment) is the knowledge of the average value of material coefficients as a function of aging time after heat treatment. For this reason, the determined average values of the material coefficients for the tested strain hardening models as a function of the natural aging time after heat treatment are summarized in Table 2.

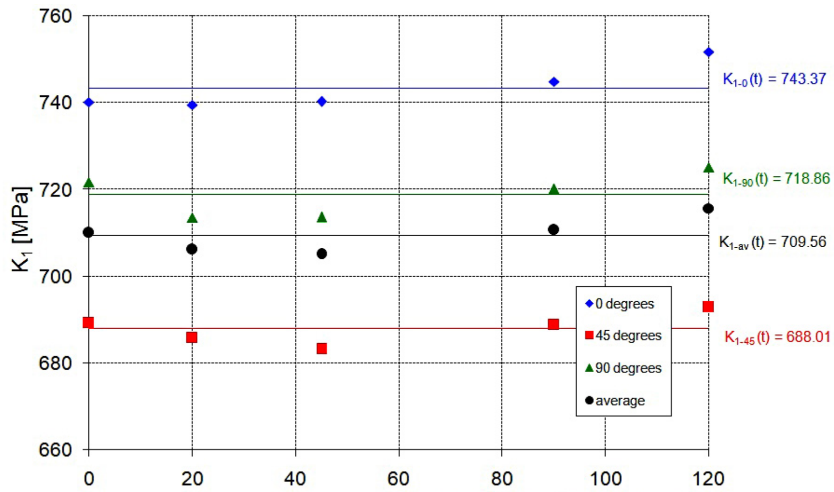

Fig. 10. Influence of aging time on the K_1 parameter in the Hollomon equation

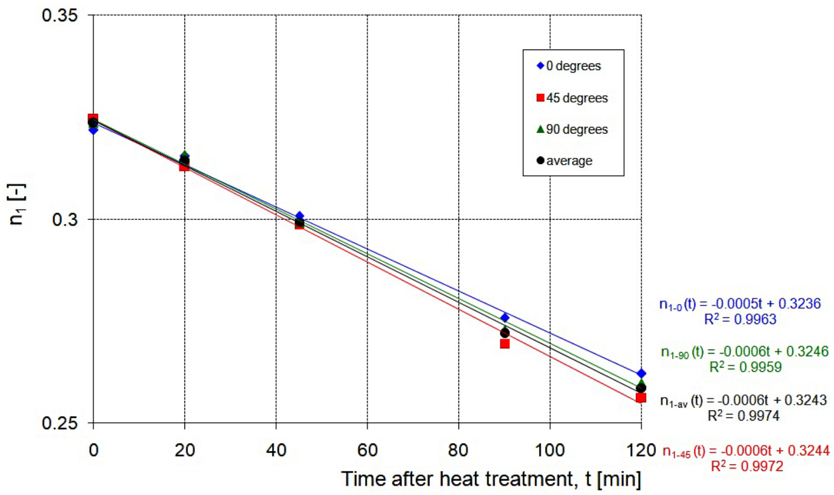

Fig. 11. Influence of aging time on the n_1 parameter in the Hollomon equation

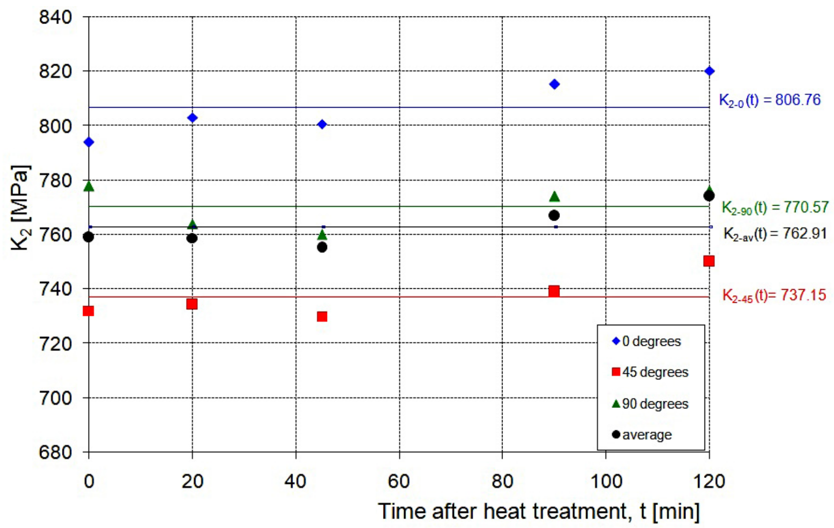

Fig. 12. Influence of aging time on the K_2 parameter in the Swift equation

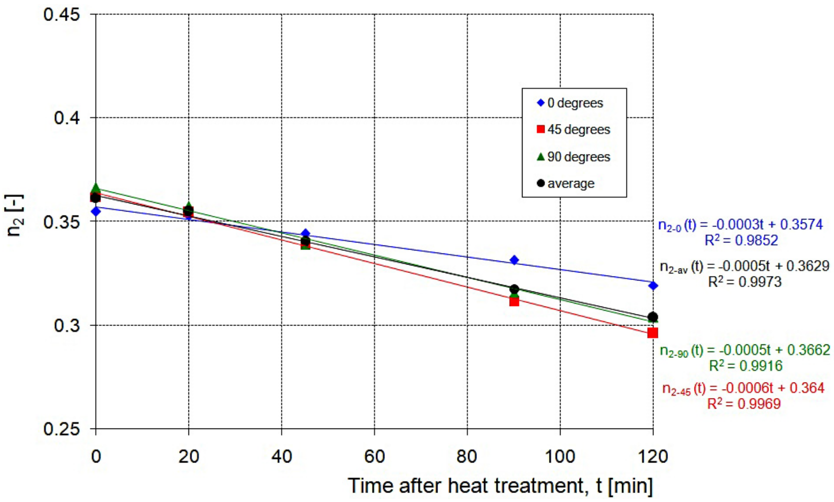

Fig. 13. Influence of aging time on the n_2 parameter in the Swift equation

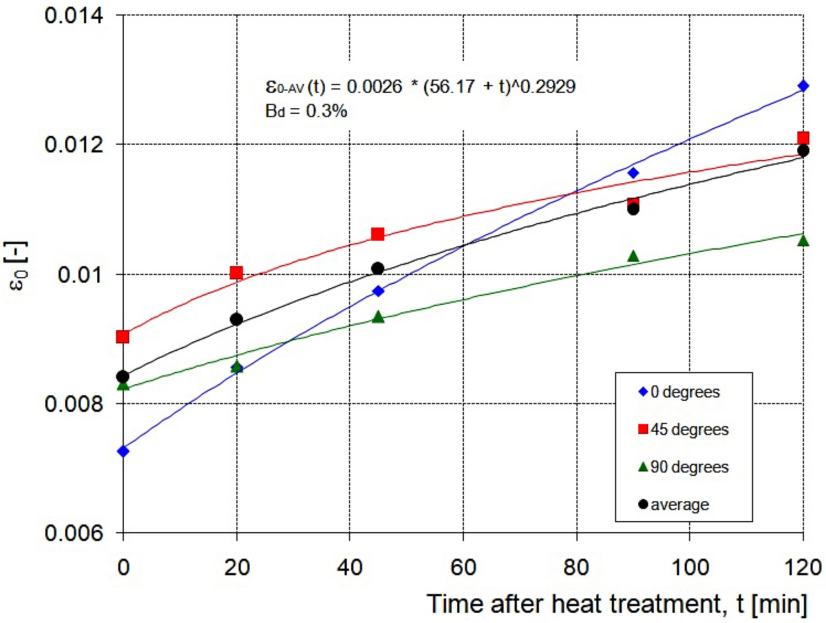

Fig. 14. Influence of aging time on the ε_0 parameter in the Swift equation

CONCLUSIONS

In this paper, constitutive parameters in the constitutive equations of flow stress as a function of natural aging time were determined on the basis of on experimental research. Based on the analysis of approximation errors, the usefulness of the tested models for describing the flow stress function of the tested sheet material after heat treatment and during natural aging in the tested time range was assessed. The aging time range for which the values of material factors were determined in excess includes the time during which individual operations of shaping the stampings from heat treatment sheets are carried out. This enables the analysis and modeling of individual stages of the molding process with the use of computer computational methods. Based on the research, the following conclusions can be drawn:

1. In the scope of the tested aging time after heat treatment 0 ÷ 120 min, an approx. 43% increase in the yield strength of the material of the tested sheet was found. Moreover, in the examined period of natural aging, the increase in the yield point was almost linear (correlation coefficient $R^2 > 0.99$).
2. Among the examined models of flow stress, the El-Magd model ($B_{d-av} \approx 0.67\%$) and the Voce model ($B_{d-av} \approx 0.83\%$) turned out to be the most accurate. The popular Swift model

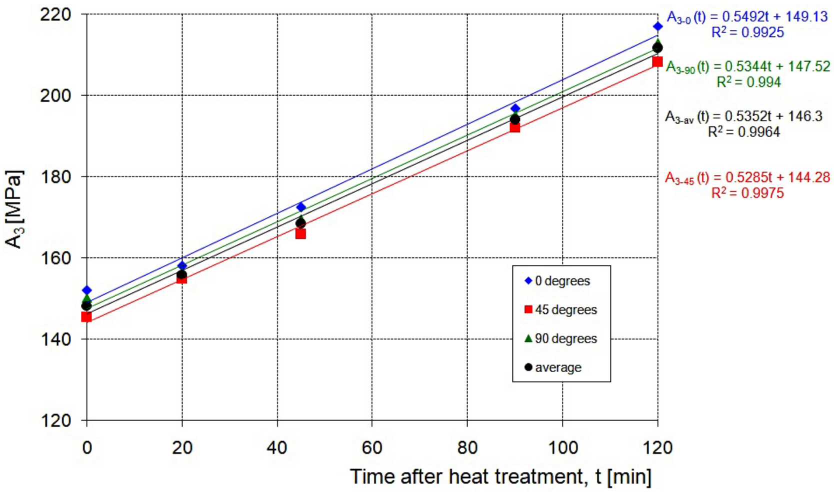

Fig. 15. Influence of aging time on the A_3 parameter in the Voce equation

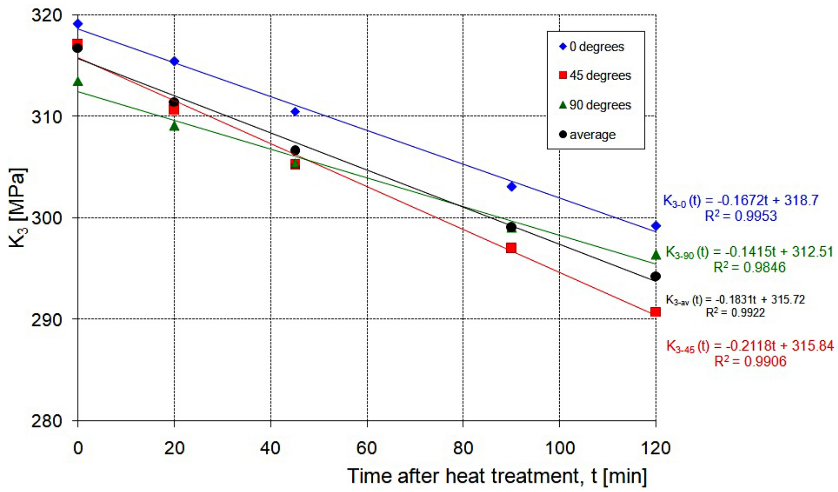

Fig. 16. Influence of aging time on the K_3 parameter in the Voce equation

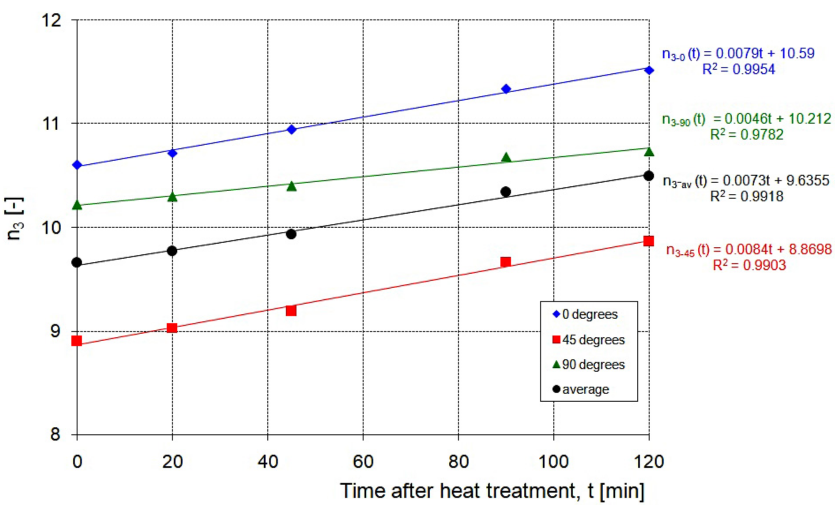

Fig. 17. Influence of aging time on the n_3 parameter in the Voce equation

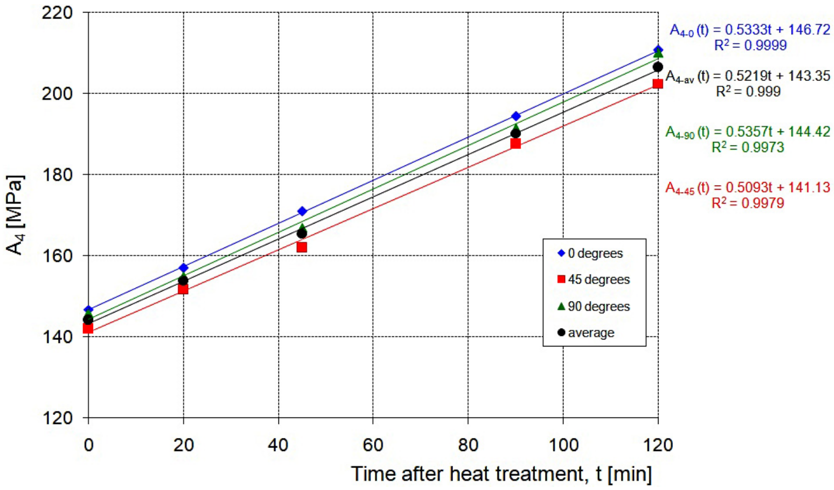

Fig. 18. Influence of aging time on the A_4 parameter in the El-Magd equation

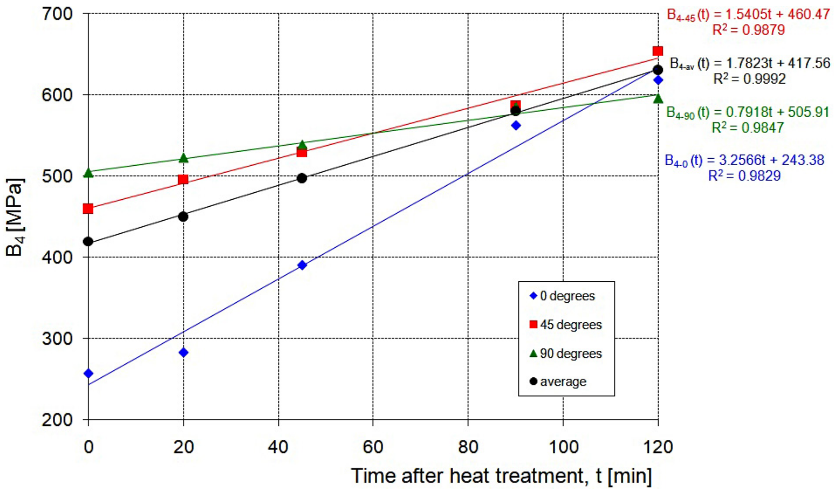

Fig. 19. Influence of aging time on the B_4 parameter in the El-Magd equation

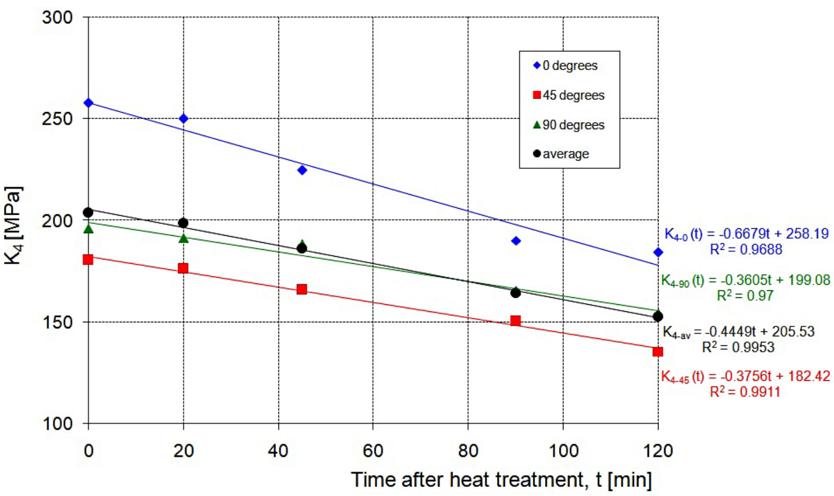

Fig. 20. Influence of aging time on the K_4 parameter in the El-Magd equation

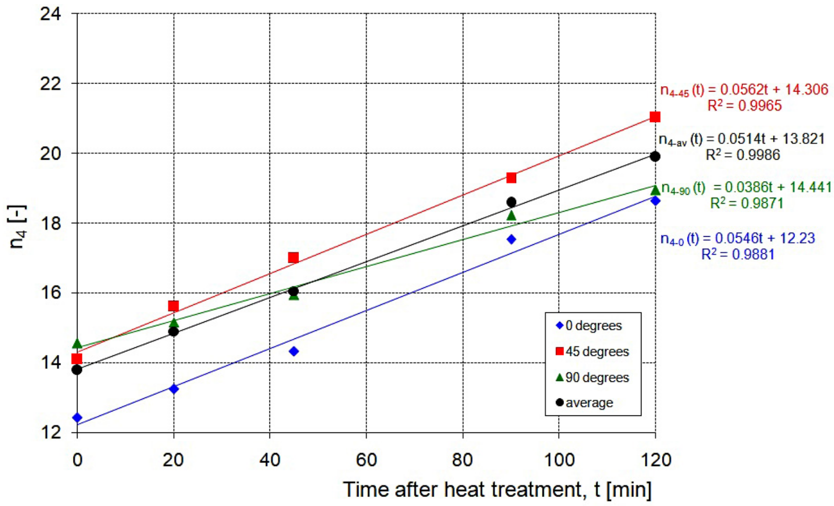

Fig. 21. Influence of aging time on the n_4 parameter in the El-Magd equation

Table 2. Experimentally determined constitutive parameters as a function of natural aging time in the range of 0–120 minutes after heat treatment for material of the tested sheet

Flow stress model		Constitutive parameters as a function of aging time after heat treatment	Average value of the parameter from the three directions	Correlation coefficient R^2
I	Hollomon	K_1(t), MPa	709.56	-
		n_1(t), -	-0.0006t + 0.3243	0.9974
II	Swift	K_2(t), MPA	762.91	-
		ε_0(t), -	0.0026*(56.17+t)^0.2929	B_d = 0.3 %
		n_2(t), -	-0.0005t + 0.3629	0.9973
III	Voce	A_3(t), MPa	0.5352t + 146.3	0.9964
		K_3(t), MPa	-0.1831t + 315.72	0.9922
		n_3(t), -	0.0073t + 9.6355	0.9918
IV	El-Magd	A_4(t), MPa	0.5219t + 143.35	0.999
		B_4(t), MPa	1.7823t + 417.56	0.9992
		K_4(t), MPa	-0.4449t + 205.53	0.9953
		n_4(t), -	0.0514t + 13.821	0.9986

was comparable ($B_{d-av} \approx 0.88\%$). It was observed that in the case of the El-Magd and Voce models, the error of matching increased with the aging time, while in the case of the Swift model it was the other way round, i.e., it decreased with aging time. In the case of the Hollomon model, the average error of matching was the highest and amounted to $B_{d-av} \approx 1,7\%$.

3. In the studied range of aging, no clear trends were found in the course of the strain hardening factor K_1 in the Hollomon model and K_2 in the Swift model as a function of the aging time. For this reason, the average value for these parameters from individual trials was adopted. The remaining parameters in the tested strain hardening models showed a clear change in the aging time function, and their course was described with the use of linear equations, except for the ε_0 parameter in the Swift model, the course of which was described by a power equation.
4. The knowledge of the constitutive parameters in the equations of flow stress on the versus time after heat treatment allows to easily take into account the change in technological properties of the material as a result of aging during the analysis and design of the plastic working processes in the second variant, i.e., after heat treatment.

REFERENCES

1. Polmear I. Light alloy – from traditional alloys to nanocrystals. Butterworth-Heinemann, Oxford, 2006.
2. Davies G. Materials for automobile bodies. Butterworth-Heinemann, Oxford, 2003.
3. Kučera V., Vojtěch D. Influence of the heat treatment on corrosion behavior and mechanical properties of the AA 7075 alloy. Manufacturing Technology. 2017; 17: 747–752.
4. Miller W.S., Zhuang L., Bottema J., Wittebrood A.J., Smet P.D., Haszler A. et al. Recent development in aluminium alloys forthe automotive industry. Composites Science and Technology. 2000; 280(1): 37–49.
5. May A., Belouchrani M.A., Taharboucht S., Boudras A. Influence of heat treatment on the fatigue behaviour of two aluminium alloys 2024 and 2024 plated. Procedia Engineering. 2010; 2: 1795–1804.
6. Sun S., Fang Y., Zhang L., Li C., Hu S. Effects of aging treatment and peripheral coarse grain on the exfoliation corrosion behaviour of 2024 aluminium alloy using SR-CT. Journal of Materials Research and Technology. 2020; 9: 3219–3229.
7. ASM Handbook. Heat Treating of Aluminum Alloys. ASM Handbook Committee 1991; 4: 841–879. DOI: 10.1361/asmhba0001205
8. Przybyłowicz K. Metaloznawstwo. WNT Warszawa, 2007. (in Polish)
9. Sobotka J., Solfronk P., Kolnerova M., Korecek D. Influence of technological parameters on ageing of aluminium alloy AW-2024. Manufacturing Technology. 2018; 18(6): 1023–1028.
10. Fallah Tafti M., Sedighi M., Hashemi R. Effects of natural ageing treatment on mechanical, microstructural and forming properties of Al 2024 aluminum alloy sheets. Iranian Journal of Materials Science & Engineering. 2018; 15(4): 1–10. DOI: 10.22068/ijmse.15.4.1
11. EN 573-3. Aluminium and aluminium alloys – Chemical composition and form of wrought products – Part 3: Chemical composition and form of products. 2007: 9.
12. AMS2770. Heat Treatment of Wrought Aluminum Alloy Parts, Rev. 2015-09.
13. Hollomon J.H. Tensile deformation. Trans. AIME. 1945; 162: 268.
14. Swift H.W. Plastic instability under plane stress. Journal of the Mechanics and Physics of Solids. 1952; 1(1): 1–18.
15. Voce E. The relationship between stress and strain for homogeneous deformations. Journal of the Institute of Metals. 1948; 74: 537–562.
16. Stiebler K., Kunze H.-D., El-Magd E. Description of the flow behaviour of a high strength austenitic steel under biaxial loading by a constitutive equation. Nuclear Engineering and Design. 1991; 127(1): 85–93.
17. Sener B., Yurci M. E. Comparison of quasi-static constitutive equations and modeling of flow curves for austenitic 304 and ferritic 430 stainless steels. Acta Physica Polonica A. 2017; 131(3): 605–607.